

2. PREVIOUS WORK

2.1. TiO_2 - FeO System

Phase relations in the TiO_2 - FeO system, at liquidus temperatures and under reducing conditions, were studied by Grieve and White⁶, MacChesney and Muan⁵ and Grau⁸. Grieve and White⁶ used the differential thermal analysis (DTA) technique for the examination of the FeO - TiO_2 system. Tungsten-molybdenum thermocouples were used. Samples were contained in molybdenum crucibles, while the standard for the differential thermocouple was also molybdenum. Three heating and two cooling curves were measured for each composition studied. The samples were made up from powdered ferrous oxide and titania and were heated in a "Pythagoras"* furnace tube situated within a molybdenum-wound furnace. Heating of the samples was done either in vacuo or in a nitrogen atmosphere. The molybdenum equipment used in the experiments would have limited the partial oxygen pressures to a maximum which is indicated by the equilibrium partial oxygen pressure between molybdenum and molybdenum oxide. These partial oxygen pressures were calculated as 2.25×10^{-11} atm at $1305^\circ C$ and 1.60×10^{-8} atm at $1600^\circ C$. The samples were examined microscopically under reflected light, and X-ray diffraction analyses were done. The FeO - TiO_2 phase diagram as determined by Grieve and White⁶ is shown in Fig. 2.1. This diagram shows four different compounds: FeO , TiO_2 , $2FeO.TiO_2$ and $FeO.TiO_2$. The eutectic points are found in the system at 5, 42 and 68 mass% TiO_2 respectively. The maximum liquidus temperature within the system, that is the liquidus temperature of TiO_2 , could not be determined with certainty and was therefore indicated to be in excess of $1650^\circ C$.

MacChesney and Muan⁵ conducted phase studies in the FeO - TiO_2 system employing the quench technique. Starting materials were Fe_2O_3 and TiO_2 . The Fe_2O_3 - TiO_2 mixtures were brought close to equilibrium with the partial oxygen pressure for which iron and wüstite coexist in equilibrium. This was accomplished by pre-reacting the mixtures in iron crucibles under a nitrogen atmosphere at $1300^\circ C$. In the actual experiments the pre-reacted oxide sample was contained in an iron crucible and sealed, together with an iron-wüstite buffer, in a vitreous silica tube. The iron-wüstite buffer was maintained at a temperature $\pm 20^\circ C$ below the sample temperature so that the partial oxygen pressure of the gas phase, as defined by the metallic iron-wüstite equilibrium, was slightly lower than that defined by the iron-wüstite buffer at the sample temperature. The partial oxygen pressure of the gas phase, calculated

* Chemical composition: SiO_2 - Al_2O_3 (approximately 67 %) Can be used at temperatures up to $1600^\circ C$

from the iron-wüstite equilibrium is approximately $10^{-10.7}$ atm at 1312°C and $10^{-9.1}$ atm at 1494°C. Some experimental runs were also made with the oxide sample contained in an iron crucible under a nitrogen atmosphere. The samples were rapidly quenched to room temperature after being held at the selected temperature until equilibrium was attained. Experimental temperatures employed were between 1250°C and 1500°C. The phases were identified by microscopic examination under reflected light, as well as X-ray diffraction analysis. The compositions of the reacted samples were determined by chemical analyses. Metallic iron was present in the quenched samples. MacChesney and Muan⁵ indicated that, according to the phase rule, iron should not be present as an equilibrium phase in their experiments. They attributed the presence of iron in the melts to the conversion of Fe_2O_3 to FeO by reaction with the iron crucible:



The FeO formed in this reaction may be reduced partially to metallic iron by the atmosphere before the FeO reacts with TiO_2 to form phases in which Fe^{2+} is stabilised. The FeO- TiO_2 phase diagram determined by MacChesney and Muan⁵ is shown in Fig. 2.2. This phase diagram has four eutectic points at 10, 47, 58 and 83 mass% TiO_2 respectively, and contains five phases: FeO, TiO_2 , $2\text{FeO} \cdot \text{TiO}_2$, $\text{FeO} \cdot \text{TiO}_2$ and $\text{FeO} \cdot 2\text{TiO}_2$.

Smith and Bell⁷ determined the solubility limit of TiO_2 in FeO at 1475°C under an argon atmosphere, using iron crucibles, to be 64.5 mass% TiO_2 .

Grau⁸ determined liquidus temperatures in the 'FeO'- TiO_2 system in the composition range of 52,7 mass% TiO_2 *-82 mass% TiO_2 . The cooling curve technique was used to determine liquidus temperatures. The melts were contained in molybdenum crucibles and a thermocouple with a molybdenum sheath was immersed in the melt. The method consisted of recording the melt temperature during cooling. The beginning of crystallisation, and therefore the liquidus temperature, is indicated by an arrest in the time-temperature curve. Experiments were conducted under argon which was deoxidised by copper turnings at 400°C. Grau⁸ maintains that the oxygen partial pressure in this argon gas was low enough to prevent oxidation of the molybdenum in the experimental apparatus. Slag analyses were determined by chemical analysis. Samples were prepared from synthetic ilmenite to which TiO_2 in the

* Ilmenite composition

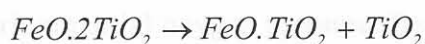
form of anatase was added in order to adjust the sample composition. The synthetic ilmenite was prepared by mixing stoichiometric amounts of pure iron, Fe_2O_3 and TiO_2 for the reaction



to occur after the mixture was pressed into pellets and reacted under argon at 1200-1300°C for ± 12 hours. X-ray diffraction confirmed the formation of ilmenite. Metallic molybdenum was found in the slags, varying between 0.6 mass% Mo for the slag containing 52.4 mass% TiO_2 and 2.2 mass% Mo for slag containing 79.5 mass% TiO_2 . Grau⁸ explains the presence of molybdenum in the slag by erosion of the molybdenum crucible by the slag and also by the solubility of molybdenum metal in the melts. The metallic molybdenum appeared as fine particles, forming a separate phase in the liquid slag melts. Therefore the chemical analysis of the melts was reported only in terms of FeO and TiO_2 after a correction was made for the molybdenum contamination.

Grau's⁸ FeO- TiO_2 phase diagram is shown in Fig. 2.3. This diagram differs from the one proposed by MacChesney and Muan⁵ for the composition range above 70 mass% TiO_2 . Grau⁸ subsequently proposed modifications to the phase diagram of MacChesney and Muan.⁵ These modifications are shown in Fig. 2.4 and include: (a) the congruent melting of pseudobrookite ($\text{FeO} \cdot 2\text{TiO}_2$) at 1475°C during which rutile and a liquid phase which contains ± 68 mass% TiO_2 are produced, and (b) eliminating the eutectic point at 83 mass% TiO_2 .

Pseudobrookite becomes unstable below $1140 \pm 10^\circ\text{C}$ ⁹, decomposing to rutile and ilmenite according to the reaction:



In a recent study of Eriksson et al.³⁵ the decomposition point was determined as $1135 \pm 5^\circ\text{C}$. Therefore, the minimum temperature in the FeO- TiO_2 phase diagram was restricted to 1200°C. According to this transformation FeO- TiO_2 slags with an overall composition between those of ilmenite and pseudobrookite will on slow cooling contain rutile in addition to ilmenite. Similarly, an ilmenite phase should be found in slowly cooled slags with a composition richer in TiO_2 than pseudobrookite. The degree to which pseudobrookite decomposes to ilmenite and rutile will be dictated by the cooling rate of the oxide mixture.

The FeO- TiO_2 phase diagram as determined by Grieve and White⁶ does not contain the $\text{FeO} \cdot 2\text{TiO}_2$ phase, as reported by MacChesney and Muan⁵. The reason for this discrepancy is

not clear. One of the photomicrographs shown in the work of Grieve and White⁶ is for 30 mass% FeO and 70 mass% TiO₂. According to MacChesney and Muan's⁵ phase diagram one would expect the sample to consist of 100% FeO·2TiO₂ at temperatures up to 1433°C and predominantly consist of FeO·2TiO₂ with a small quantity of liquid phase at temperatures from 1433°C to the liquidus temperature. Instead Grieve and White⁶ identified ilmenite and rutile. However, they did not indicate the thermal history of their samples, and therefore one assumes that the photomicrographs were produced from the samples used in the DTA studies. This explanation agrees with Lindsley's⁹ finding, as discussed by Grau⁸, that pseudobrookite is unstable below ±1140°C, and decomposes into ilmenite and rutile, the phases identified by Grieve and White⁶.

The origin of the difference between the FeO-TiO₂ phase diagrams (especially the liquidus temperatures) proposed by Grau⁸ and by MacChesney and Muan⁵ above 70 mass% TiO₂ might be that MacChesney and Muan⁵ fixed the partial oxygen pressure in their experiments, while Grau⁸ did not. Grau⁸ also states that no attempt was made to equilibrate the slags with the oxygen in the gas phase in order to avoid compositional changes in the slag and also because of the "dynamic" nature of the DTA technique. It is therefore incorrect to compare the liquidus temperatures as determined by Grau⁸ with that of MacChesney and Muan⁵ because the partial oxygen pressure in the work of MacChesney and Muan⁵ was fixed for most of their experiments whilst the partial oxygen pressure in Grau's⁸ work is uncertain and clearly higher than that of MacChesney and Muan⁵. The presence of molybdenum in the slags from Grau's⁸ work indicates a partial oxygen pressure reducing with respect to the Mo/MoO equilibrium partial oxygen pressure. Because of the similar partial oxygen pressures imposed by the Fe/FeO and Mo/MoO equilibria it is possible that significant amounts of molybdenum oxide was present in the slag. On cooling the molybdenum oxide could have decomposed to form metallic molybdenum which was found in the slags. It should be borne in mind that metallic molybdenum was also present in the slags produced by Grieve and White⁶.

Eriksson and Pelton¹² used all the available thermodynamic and phase equilibrium data to obtain a set of model equations for the Gibbs energies of all the phases, as a function of temperature and composition. A modified quasichemical model was used to represent the thermodynamic properties. Coefficients within the model were obtained by optimisation of the available data. The calculated FeO-TiO₂ diagram is shown in Fig. 2.5. The diagram agrees well with the data of Grau⁸ at high TiO₂ contents and with the diagram of MacChesney and

Muan⁵ for TiO₂ constants below 50 mol% TiO₂. Eriksson and Pelton¹² estimated the probable maximum inaccuracy in the assessed diagram to be $\pm 20^\circ\text{C}$.

2.2. FeO - VO_x System

Wakihara and Katsura¹⁰ determined phase equilibria in the FeO-Fe₂O₃-V₂O₃ system at 1227°C under various oxygen partial pressures ranging from 1.15×10^{-3} to 1.40×10^{-14} atm. This was done by using quench and thermogravimetric techniques. The quench technique consisted of equilibrating the samples in gas mixtures, of specific oxygen partial pressure, followed by quenching in cold water. The oxygen partial pressure was regulated by either a CO₂/H₂ or a CO₂/O₂ gas mixture. X-ray diffraction was used to identify the phases present in the quenched samples. The thermogravimetric method consisted of continuously weighing an oxide pellet, which was suspended from a thin platinum wire, in a vertical tube furnace. The mass changes were recorded at constant temperature as a function of time at different oxygen partial pressures. The applicable oxygen partial pressure within the furnace was measured by the use of a solid electrolyte cell with partially stabilised zirconia as the solid electrolyte. The 1227°C isothermal section of the FeO-Fe₂O₃-V₂O₃ system as determined by Wakihara and Katsura¹⁰ is shown in Fig. 2.6. Three solid solution phases can be distinguished in this system, namely a sesquioxide solid solution, a spinel solid solution and the wüstite solid solution.

Phase equilibria within the Fe-Fe₂O₃-V₂O₃ system were determined by Katsura et al.¹¹ at 1227°C under partial oxygen pressures between 1.05×10^{-9} and 3.55×10^{-14} atm. The oxide samples were contained in alumina crucibles and the experimental procedure employed was similar to that used by Wakihara and Katsura.¹⁰ Katsura et al.¹¹ did not report any contamination of samples due to the use of alumina crucibles. Fig. 2.7. shows the phase diagram determined by Katsura et al.¹¹. The diagram indicates that the M₃O₄ solid solution, with composition ranging from that of Fe₃O₄ to the composition point B, is in equilibrium with vanadowüstite on line (C)-(E). However, the M₃O₄ solid solution phase from composition point B to FeV₂O₄ is in equilibrium with metallic iron. This phase diagram corresponds with the phase diagram of Wakihara and Katsura¹⁰ in that both contain the spinel solid solution phase between FeV₂O₄ and Fe₃O₄, the wüstite phase field and the corresponding two phase and three phase fields between the spinel solid solution, wüstite and iron.

Schmahl and Dillenburg¹⁴ equilibrated condensed phase mixtures with CO/CO₂ gas mixtures at 900°C. The gas mixture was pumped in a closed loop over the condensed phase until

equilibrium was attained. The CO/CO₂ ratio was analysed in situ and a ternary phase diagram was constructed from the data as shown in Fig. 2.8. The phases Fe₂O₃, V₂O₃, Fe, FeO_{1.04} and FeV₂O₄ were identified.

General agreement exists between Wakihara and Katsura¹⁰, Katsura e.a.¹¹ and Schmahl and Dillenburg¹⁴ on phase relations in the iron-rich corner of the Fe-V-O system. These phase relations cover the temperature range of 850°C to 1227°C and indicates that the spinel and sesquioxide solid solutions are to be expected above 1227°C because these are phases of high melting temperatures and spinels are stable up to high temperatures.

2.3. TiO₂ - VO_x System

The only TiO₂-VO_x phase diagram which could be obtained from the literature is the TiO₂-VO₂ phase diagram¹⁵ in the temperature range of 27-107°C. This diagram is however of little value to the present study.

2.4. TiO₂ - VO_x - FeO_y System

The ternary phase diagram TiO₂-V₂O₅-Fe₂O₃ is known at temperatures below 700°C, as is shown in Fig. 2.9.¹⁶ Although V₂O₅ and Fe₂O₃ are not stable at the oxygen potentials employed in the present study, the ternary diagram serves as a reference point as to the type of phases to be expected. These are phases similar to FeVO₄, Fe₂V₄O₁₃ in the FeO-VO_x system and Fe₂TiO₅ in the TiO₂-FeO system. No other phase studies within the TiO₂-VO_x-FeO_y ternary system could be found in the literature.

2.5. TiO₂ - Ti₂O₃ System

Eriksson and Pelton¹² constructed an optimised phase diagram of the TiO₂-Ti₂O₃ system as is shown in Fig. 2.10. As for the FeO-TiO₂ diagram discussed in 2.1, a modified quasichemical model was used to represent the thermodynamic properties and the coefficients within the model were obtained by optimisation of the available data. The system contains the compound Ti₃O₅ with a pseudobrookite structure, and a series of defect compounds known as Magneli phases.

Magneli phases are crystallographic shear structures represented by the general formula Ti_nO_{2n-1} for Ti-O mixtures.²¹ The phases with 4 ≤ n ≤ 10 have crystal structures derived from the rutile structure.¹² Phases with n > 10 have structures based on other shear planes and so

form different families of phases.²¹ For Magneli phases consisting of Ti and O the largest value for n has been estimated to be as high as 99. However, according to Murray and Wriedt²¹ the lower estimates for the value of n are more realistic because these estimates are based on structural data.

Eriksson and Pelton¹² relied heavily on the work of Zador and Alcock²⁰ in constructing the phase diagram in Fig. 2.10. For the higher Magneli phases n was arbitrarily set equal to 20, and all of the higher Magneli phases are represented by $Ti_{20}O_{39}$ on the diagram. The probable maximum inaccuracy in the optimised Ti_2O_3 - TiO_2 diagram of Eriksson and Pelton¹² is estimated by them as ± 20 °C for mole fraction TiO_2 in excess of 0.4.

2.6. Conclusion

From the literature reviewed in 2.1 to 2.5 it is evident that only a small amount of data is available on phase relations in the TiO_2 - FeO_Y - VO_Z pseudo-ternary system. Although the TiO_2 - FeO binary system has been studied in detail by a number of researchers, considerable disagreement exists between their reported results. These differences in reported phase relation data can be explained by differences in experimental procedures employed in the different studies. The only recent study on the high TiO_2 side of the TiO_2 - FeO pseudo binary system is the study made by Du Plooy³⁶ employing a thermal analysis technique, similar to that of Grau.⁸ The maximum temperature at which phase relations in the FeO - V_2O_3 - Fe_2O_3 ternary system is known is 1227°C¹⁰. Phase relations in the FeO - V_2O_3 binary system are available from the FeO - V_2O_3 - Fe_2O_3 system. Therefore considerable room exists for phase relation determinations in the FeO - V_2O_3 system at temperatures above 1227°C. No data could be found on the TiO_2 - VO_x binary system, or the TiO_2 - FeO_Y - VO_Z pseudo-ternary system at relevant oxygen partial pressures. Therefore there is great need for data on phase relations in the pseudo-binary phase diagrams which constitute the TiO_2 - FeO_Y - VO_Z pseudo-ternary system, as well as in the TiO_2 -rich side of this pseudo-ternary system.

Fig. 2.1: FeO-TiO₂ Phase Diagram: Grieve and White⁶

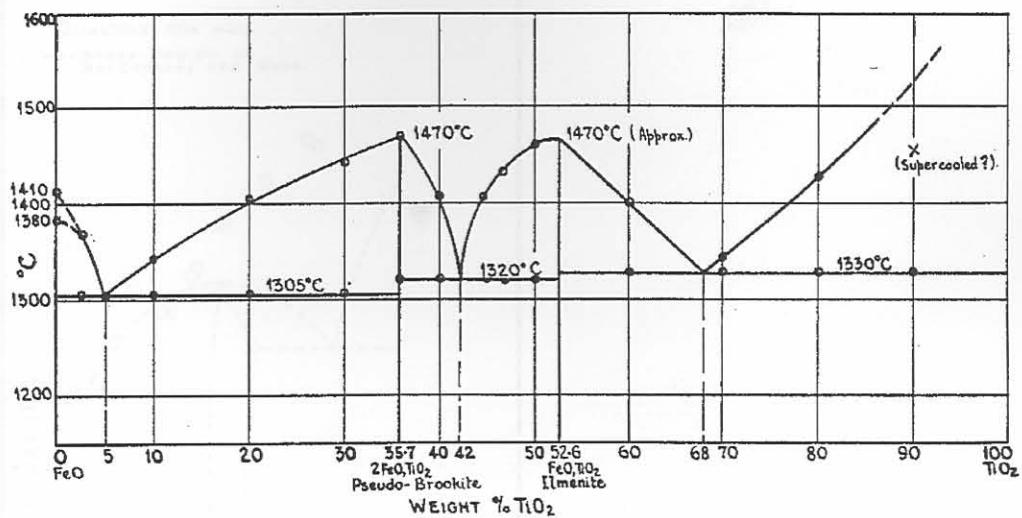


Fig. 2.2: FeO-TiO₂ Phase Diagram: MacChesney and Muan⁵

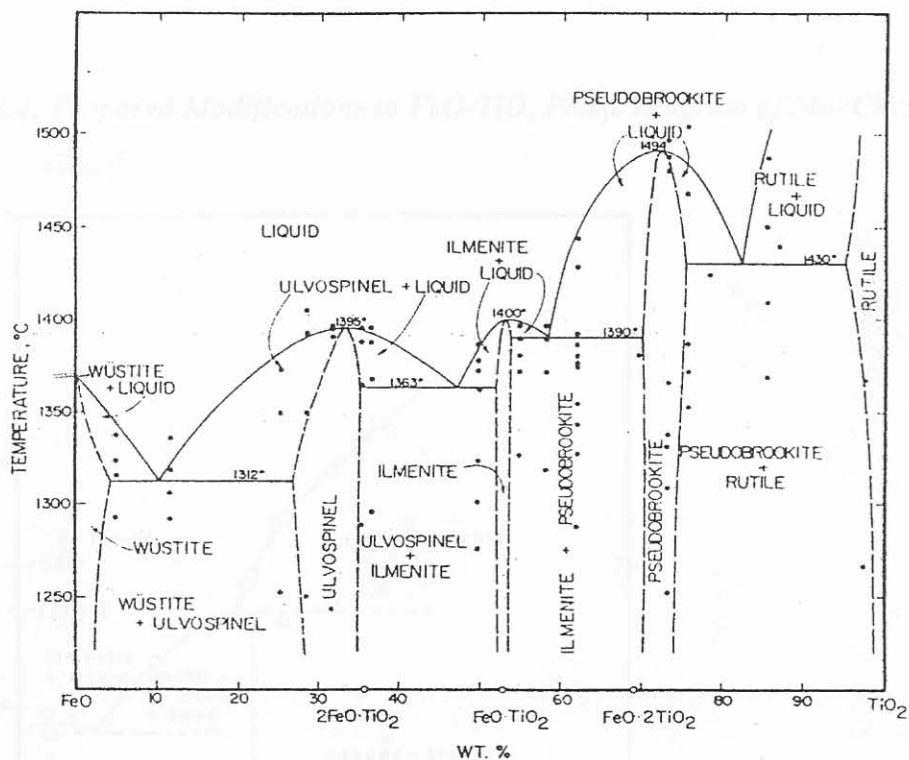


Fig. 2.3: Liquidus Temperature Measurements in FeO-TiO₂ System: Grau⁸

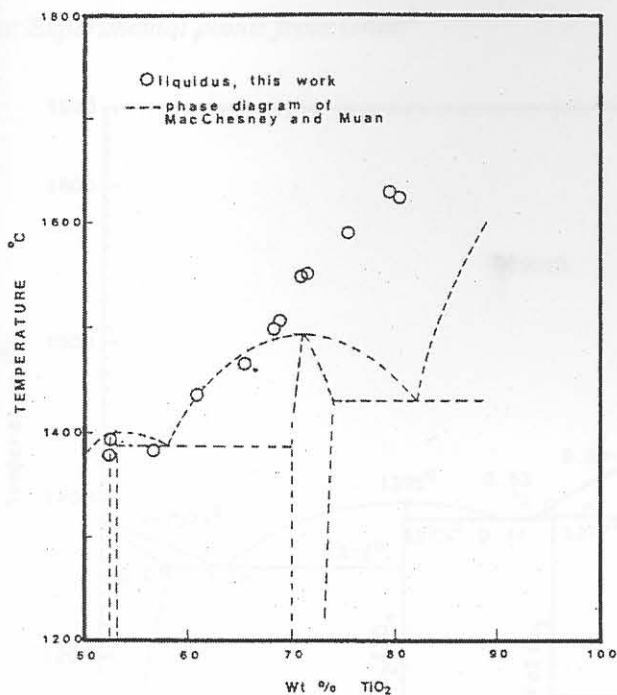


Fig. 2.4: Proposed Modifications to FeO-TiO₂ Phase Diagram of MacChesney and Muan⁵
 : Grau⁸

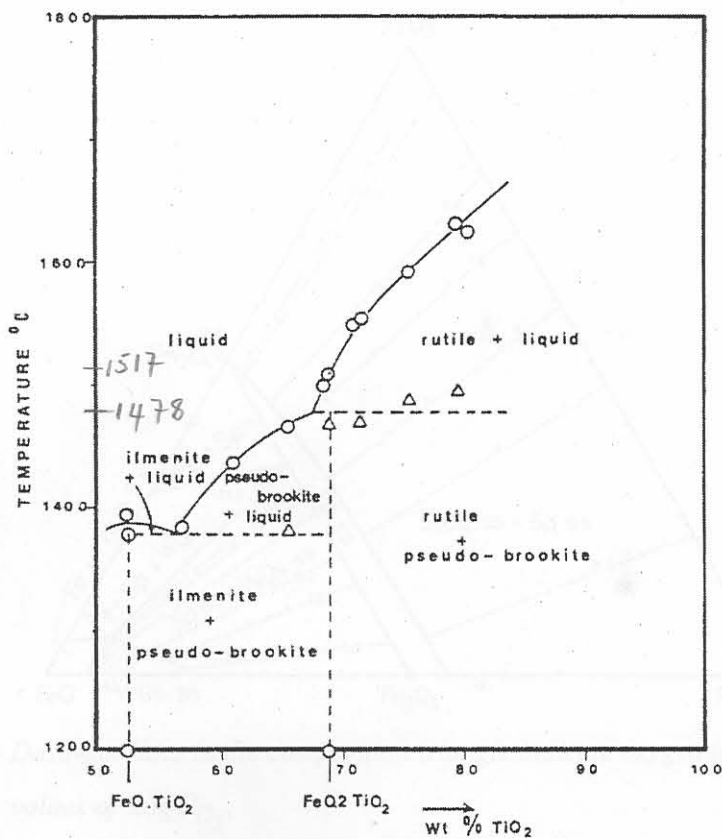


Fig. 2.5: Optimised FeO-TiO₂ Phase Diagram: Eriksson and Pelton¹²

o: Experimental points from Grau⁸

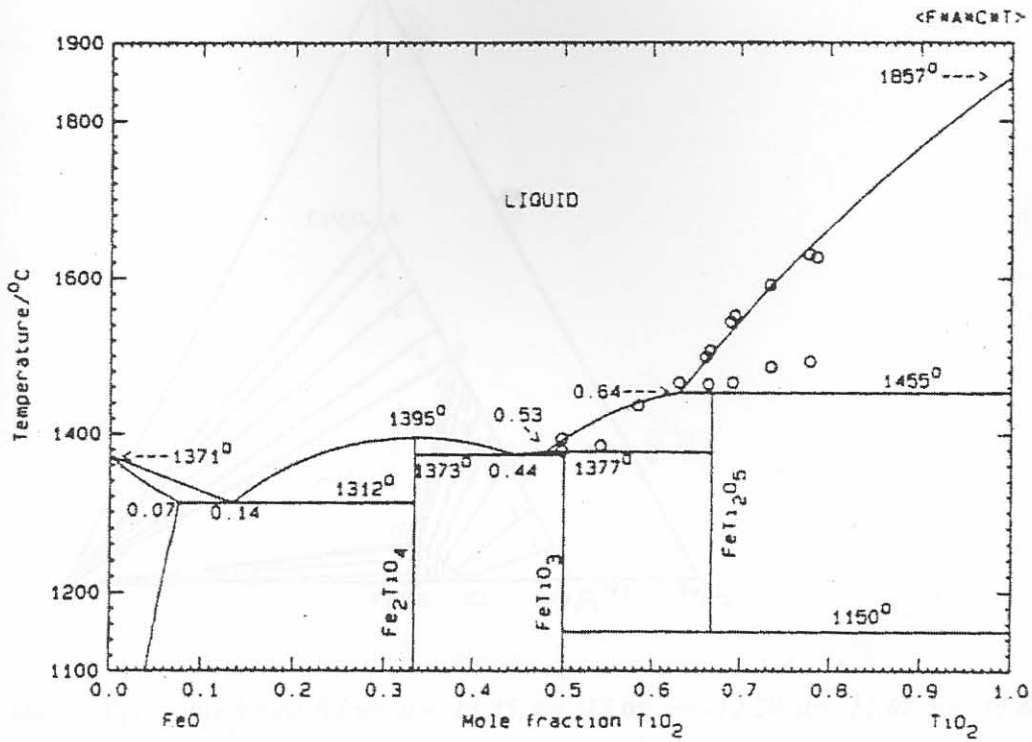
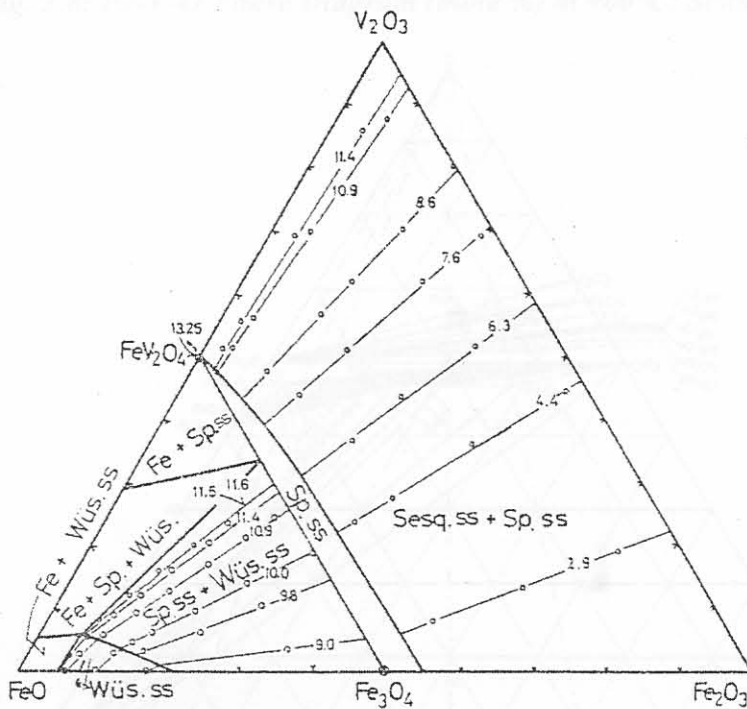
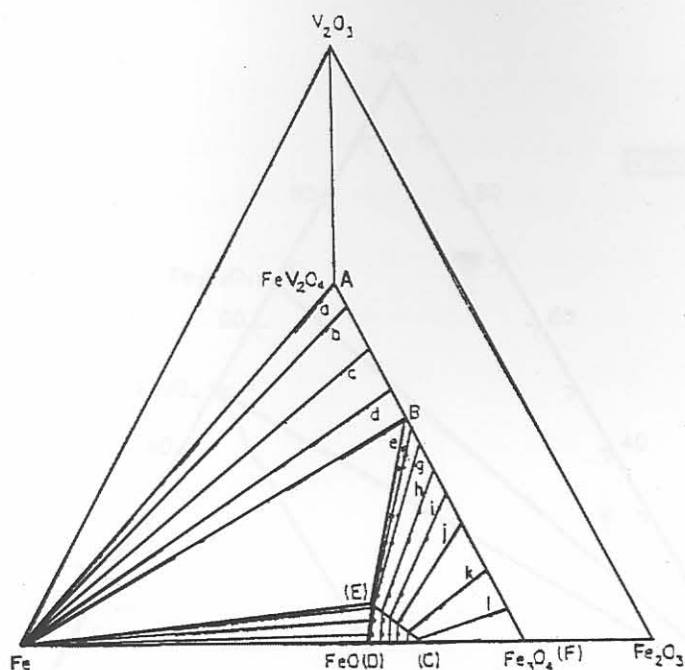


Fig. 2.6: FeO-Fe₂O₃-V₂O₃ Phase Diagram (mole %) at 1227°C: Wakihara and Katsura¹⁰



Dash-dot lines in the composition triangle indicate oxygen isobar and numbers on the lines are values of $-\log P_{O_2}$.

Fig. 2.7: Fe-Fe₂O₃-V₂O₃ Phase Diagram (mole %) at 1227°C: Katsura et al¹¹



The log P_{O_2} value for each line: a = -13.45, b = -12.69, c = -12.20, d = -11.87, e = -11.68, f = -11.56, g = -11.37, h = -10.83, i = -10.45, j = -10.03, k = -9.39, l = -8.98.

B: 42.80% Fe₂O₃, 20.00% Fe, 37.20% V₂O₃; E: 51.60% Fe₂O₃, 41.70% Fe, 6.70% V₂O₃.

Fig. 2.8: Fe-V-O Phase Diagram (mole %) at 900°C: Schmahl and Dillenburgh¹⁴

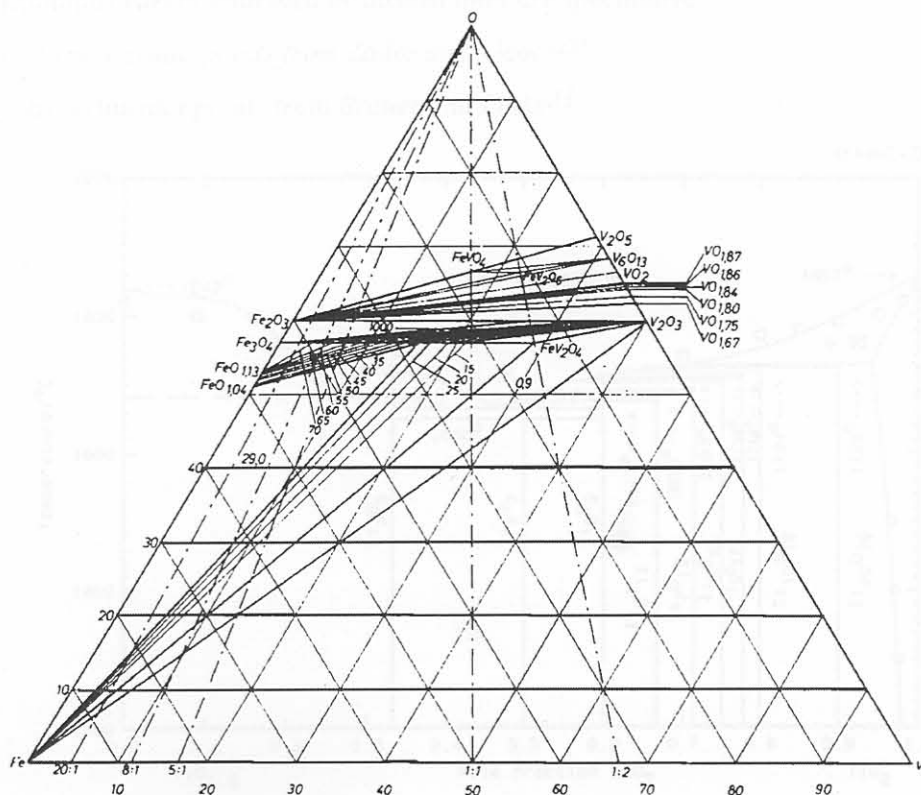


Fig. 2.9: TiO_2 - V_2O_5 - Fe_2O_3 Phase Diagram: Fotiev et al¹⁶

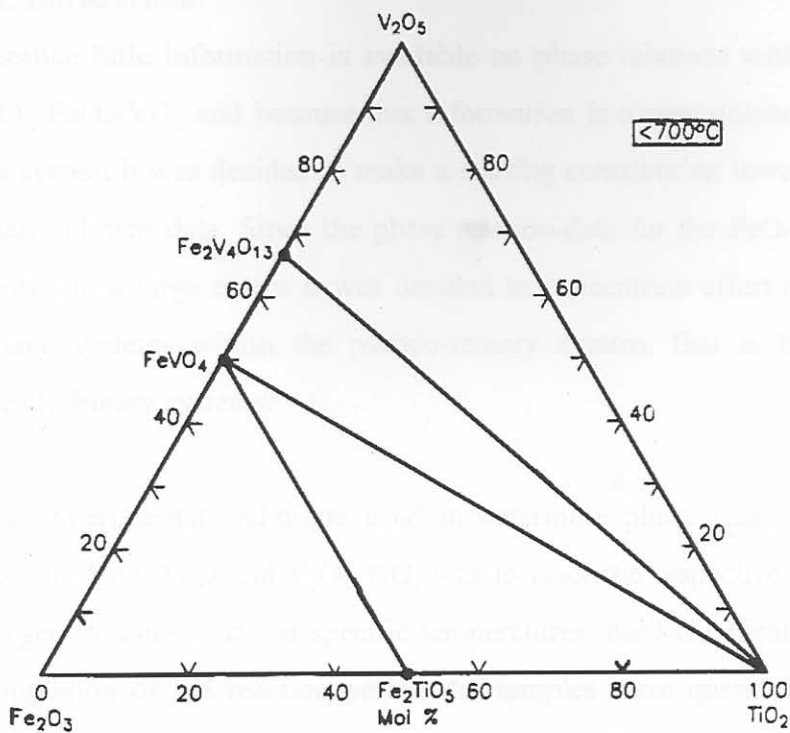


Fig. 2.10: Ti_2O_3 - TiO_2 Phase Diagram: Eriksson and Pelton¹²

(Liquidus curves indicated by dashed lines are speculative)

o: Experimental points from Zador and Alcock²⁰

□: Experimental points from Brauer and Littke³¹

